

- for lock-in detection. The effective electron base temperature, $T_{\text{base}} \approx 45$ mK, was measured from CB peak widths in the weak tunneling regime.
15. N. E. Bickers, *Rev. Mod. Phys.* **59**, 845 (1987).
 16. The presence of more than one state in our dots is expected to enhance the Kondo temperature. For an analysis of multiple-level effects, see T. Inoshita *et al.*, *Phys. Rev. B* **48**, 14725 (1993); T. Inoshita, Y. Kuramoto, H. Sakaki, *Superlattices Microstruct.* **22**, 75 (1997); T. Pohjola *et al.*, *Europhys. Lett.* **40**, 189 (1997).
 17. E. B. Foxman *et al.*, *Phys. Rev. B* **47**, 10020 (1993).
 18. The dI/dV minimum of valley 4 resembles the form predicted by J. König, H. Schoeller, and G. Schön [*Phys. Rev. Lett.* **76**, 1715 (1996)] for a quantum dot with $N = \text{even}$.
 19. Our data fit well to the theoretical predictions when we use the g factor for bulk GaAs, $g = -0.44$, whereas the g factor in the 2DEG of a typical GaAs/AlGaAs heterostructure has been experimentally determined to be less than in the bulk by M. Dobers, K. v. Klitzing, and G. Weimann [*Phys. Rev. B* **38**, 5453 (1988)].

20. We thank R. Aguado, B. Broer, L. I. Glazman, S. F. Godijn, K. K. Likharev, C. M. Marcus, J. E. Mooij, and N. C. van der Vaart for help and discussions and Philips Laboratories and C. T. Foxon for providing the heterostructure. Supported by the Dutch Foundation for Fundamental Research on Matter (FOM), the Royal Netherlands Academy of Arts and Sciences (L.P.K.), and the NSF under grant DMR-945805 (S.M.C.).

30 March 1998; accepted 2 June 1998

Mass-Independent Oxygen Isotope Fractionation in Atmospheric CO as a Result of the Reaction $\text{CO} + \text{OH}$

T. Röckmann, C. A. M. Brenninkmeijer, G. Saueressig, P. Bergamaschi, J. N. Crowley, H. Fischer, P. J. Crutzen

Atmospheric carbon monoxide (CO) exhibits mass-independent fractionation in the oxygen isotopes. An ^{17}O excess up to 7.5 per mil was observed in summer at high northern latitudes. The major source of this puzzling fractionation in this important trace gas is its dominant atmospheric removal reaction, $\text{CO} + \text{OH} \rightarrow \text{CO}_2 + \text{H}$, in which the surviving CO gains excess ^{17}O . The occurrence of mass-independent fractionation in the reaction of CO with OH raises fundamental questions about kinetic processes. At the same time the effect is a useful marker for the degree to which CO in the atmosphere has been reacting with OH.

Small variations in isotopic composition occur throughout nature and often give useful information about physical, chemical, and biological processes. The various underlying isotope fractionation effects are normally proportional to isotopic mass differences (1); however, isotope fractionation effects have recently been discovered that do not depend on the mass of the substituted isotope (2–10). The causes of the sometimes exceptionally strong mass-independent fractionation (MIF) are complex and not yet understood. In the atmosphere MIF is widespread, and each of the important trace gases— O_3 (2, 6), CO_2 (7), CO (5, 8, 9) and N_2O (10)—has excess ^{17}O , which for oxygen is an excellent marker for MIF. The clearest case of MIF occurs in atmospheric O_3 , in which both ^{17}O and ^{18}O are nearly equally enhanced relative to its precursor, atmospheric O_2 . This is in contrast to most other oxygen-bearing compounds on Earth for which $\delta^{17}\text{O} = 0.52 \times \delta^{18}\text{O}$ (11). For MIF, $\Delta^{17}\text{O} \equiv \delta^{17}\text{O} - 0.52 \times \delta^{18}\text{O} \neq 0$.

MIF in CO was discovered from analysis of samples collected in New Zealand (8). Subsequent measurements established that it is a widespread phenomenon, and initially the

effect was linked to MIF in O_3 (5). The reaction of O_3 with unsaturated hydrocarbons, mainly isoprene and terpenes emitted by plants, indeed produces CO that inherits the relatively strong MIF in O_3 of 25 to 40 per mil (5, 6). However, despite the large $\Delta^{17}\text{O}(\text{O}_3)$ value, there is insufficient CO from this source to explain the observed $\Delta^{17}\text{O}(\text{CO})$ values in remote air masses (5).

Our measurements reveal that $\Delta^{17}\text{O}(\text{CO})$ values at high northern latitudes vary seasonally (Fig. 1). In winter, CO in clean surface air at Alert and Spitsbergen peaks at about 170 ppb. Removal rates for reaction with hydroxyl (OH) are low, the sources outweigh the sink, and the isotopic composition of the accumulating CO reflects that of the combined sources. Because fossil fuel combustion is an important source of CO, $\delta^{18}\text{O}$ values are high (12) and $\Delta^{17}\text{O}(\text{CO})$ values are low (5). During spring and summer, oxidative cleaning of the atmosphere by OH gathers momentum and CO levels decline. Concurrently $\delta^{18}\text{O}$ values decrease because of the inverse kinetic isotope effect (13) and the diminished role of fossil fuel sources (12). In contrast, $\Delta^{17}\text{O}(\text{CO})$ values reach their highest levels when OH peaks in summer, implicating the reaction between CO and OH as a possible source of MIF.

To investigate MIF in this reaction, we

saturated a mixture of $\sim 1\%$ CO in He or N_2 as the bath gas with H_2O_2 vapor and circulated the mixture through a photochemical reactor in which OH was produced from photolysis of H_2O_2 with a Xe lamp (wavelength $\lambda > 190$ nm). After a reaction time of 15 to 90 min, typically 15 to 65% of the original CO had been oxidized, and the residual CO was analyzed for its $^{13}\text{C}/^{12}\text{C}$ and $^{18}\text{O}/^{16}\text{O}$ ratio by mass spectrometry (12, 14). For $^{17}\text{O}/^{16}\text{O}$ analysis, samples were first converted to O_2 with a F_2 -based technique (15). With this method $^{17}\text{O}/^{16}\text{O}$ variations can be resolved from the strongly interfering $^{13}\text{C}/^{12}\text{C}$ variations. The results show that the remaining CO fraction progressively obtains excess ^{17}O (Fig. 2). The effect diminishes at lower pressures and also when He is used as a bath gas. The equilibrium fractionation, plotted versus pressure in Fig. 3, was derived from the slopes of the linear fits in Fig. 2.

To ascertain that the MIF observed here exclusively arises from the chemical reaction of CO with OH, we need to exclude possible interferences. An alternative mechanism would be transfer of MIF from OH to CO through isotopic exchange. However, measurements confirm that the H_2O_2 used and consequently the OH formed is free of MIF. Furthermore, there exists experimental and theoretical evidence against significant oxygen isotope exchange in the reaction between CO and OH (16).

The generation of MIF in CO by means of exchange with OH is excluded in the troposphere as well (5). Although atmospheric OH is mainly produced by the reaction $\text{O}(^1\text{D}) + \text{H}_2\text{O} \rightarrow 2 \text{OH}$, and initially must reflect the strong MIF of O_3 [the $\text{O}(^1\text{D})$ precursor], fast exchange with H_2O according to $\text{OH} + \text{H}_2\text{O} \leftrightarrow \text{H}_2\text{O} + \text{OH}$ efficiently washes the MIF signal out (17).

Other potential interfering agents in our experiments were $\text{O}(^3\text{P})$ or $\text{O}(^1\text{D})$, which could cause MIF by exchange or reaction with CO. Whether or not O_2 is excluded from the experiments, some is inevitably produced by thermal decomposition of H_2O_2 and the photochemical reactions involving OH, HO_2 , and H_2O_2 . Experiments with the addition of 10 to 20% O_2 , with and without H_2O_2 , confirm that MIF in the remaining CO only occurs when H_2O_2 is present.

An independent check on our experiments

Max Planck Institute for Chemistry, Atmospheric Chemistry Division, Postfach 3060, 55020 Mainz, Germany.

is that the ^{13}C and ^{18}O measurements agree well (Fig. 3) with earlier data (13, 18). The ^{13}C values show a positive kinetic isotope effect of 6 per mil at atmospheric pressure, turning into a negative isotope effect below 400 mbar. For ^{18}O , a negative kinetic isotope effect of -10 per mil with little pressure dependence is observed. Note that all three isotope fractionation processes and the overall rate constant of $\text{CO} + \text{OH}$ [$k = 1.5 \times 10^{-13} \times (1 + 0.6 \times p_{\text{atm}}) \text{ cm}^3 \text{ molecule}^{-1} \text{ s}^{-1}$ (19)] exhibit different pressure dependencies. From the above arguments we conclude that the observed MIF in the remaining CO is solely caused by differences in net reaction rate coefficients of the different CO isomers with OH.

Can the measurements explain the atmospheric $\Delta^{17}\text{O}$ observations? The $\Delta^{17}\text{O}$ data from Fig. 3 apply to the case in which CO sources and sinks are at a steady state. This situation does not occur in the atmosphere but is best approached in the tropics and subtropics, where OH concentrations vary moderately over the seasons. At Izaña (Tenerife, 28°N) CO levels were nearly constant during winter (Fig. 1). For 750 mbar, corresponding to the

station's altitude, the predicted $\Delta^{17}\text{O}$ value is 4.2 ± 0.3 per mil (Fig. 3), which agrees with the observations (Fig. 1).

At high northern latitudes, CO sources and the OH-based sink never approach steady state because of the strong seasonality in OH concentrations. In fall and winter, CO sources dominate the weakened OH sink, and the observed decline of $\Delta^{17}\text{O}$ to 2.5 per mil in late February can be quantitatively explained by dilution of the CO reservoir with mass-dependently fractionated CO from combustion (5). In spring and summer, $\Delta^{17}\text{O}$ exceeds the equilibrium fractionation value because the OH sink is stronger than the combined CO sources. Essentially, reaction with OH reduces the CO inventory to about 45% of the winter levels (Fig. 1). Figure 2 shows that such a reduction of CO [$\ln(\text{remaining CO}) = -0.80$] yields a $\Delta^{17}\text{O}$ shift of 3.5 per mil, which adds to the winter minimum of 2.5 per mil.

The actual situation is complicated by the continuous input of CO from various sources. If we start with a given CO reservoir with $\Delta^{17}\text{O} = 2.5$ per mil, again reduce it to 45% of the starting level but now include a source, even more CO must react with OH. Therefore, final $\Delta^{17}\text{O}$ values are higher than in the no-source scenario (although the source has $\Delta^{17}\text{O} = 0$) and can reach up to 7 per mil depending on the source strength, which we varied between 0.5 and 1.5 ppb per day. Thus, the reaction of CO with OH can produce $\Delta^{17}\text{O}$ values between 6 and 7 per mil at high northern latitudes in late summer. The small difference relative to the observed values (Fig. 1) can easily be accounted for by a moderate contribution (2 to 6% in summer) from the ozonolysis source (5).

By calculating the altitude-weighted integral of CO, OH, $k_{\text{CO}+\text{OH}}$ and $\Delta^{17}\text{O}$ for the CO + OH reaction, we can estimate that $\Delta^{17}\text{O} = 4.2 \pm 0.3$ per mil is a representative value for the entire troposphere in source-to-sink equilibrium. This value corresponds to

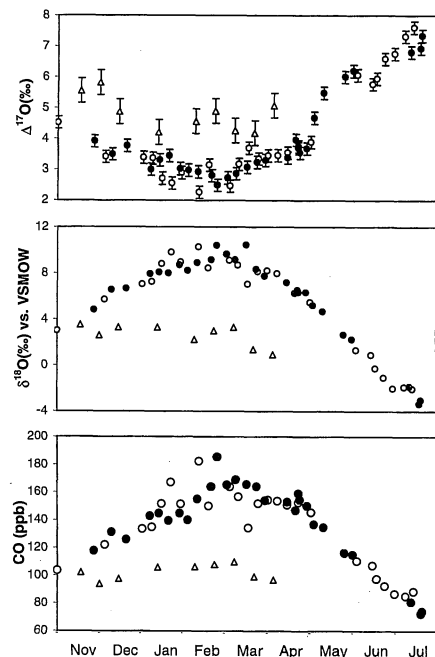


Fig. 1. $\Delta^{17}\text{O}(\text{CO})$ and $\delta^{18}\text{O}(\text{CO})$ values (in per mil), and CO mixing ratios measured for air collected at Alert (Canada, 81°N , open circles), Spitsbergen (79°N , solid circles), and Izaña (Tenerife, 28°N , triangles) in 1996 and 1997. At high northern latitudes, CO and $\delta^{18}\text{O}(\text{CO})$ peak in winter, when ^{18}O -enriched CO from fossil fuel combustion is more abundant. In summer, reaction with OH, which preferentially removes C^{18}O , is most important, and CO and $\delta^{18}\text{O}$ are low. In contrast, $\Delta^{17}\text{O}(\text{CO})$ bottoms out in winter and reaches its maximum in summer. The 1σ errors for CO and $\delta^{18}\text{O}$ fall within the data symbols.

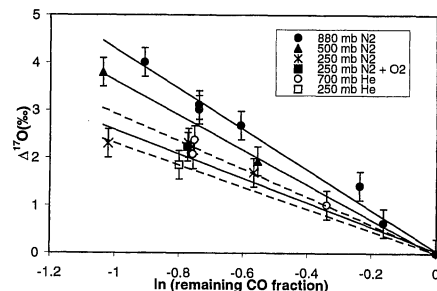
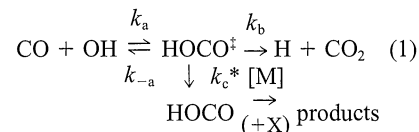


Fig. 2. The excess ^{17}O enrichment in CO resulting from reaction with OH is shown as $\Delta^{17}\text{O}$ relative to the original CO with $\Delta^{17}\text{O} = 0$ versus the natural logarithm of the remaining CO fraction. Solid lines are linear fits to the data obtained with the bath gas N_2 , dashed lines with He.

an effective altitude of ~ 750 mbar (Fig. 3). In the upper troposphere the MIF is less, but also considerably less CO is being destroyed there.

The CO + OH reaction involves an association complex HOCO^\ddagger (20–22) in a vibrationally excited state ($[M]$ is the bath gas concentration).



In steady state, the overall rate constant can be expressed as

$$k = k_a \frac{k_b + k_c[M]}{k_{-a} + k_b + k_c[M]} \quad (2)$$

This scheme shows that any fractionation in the HOCO^\ddagger formation step (a) does not depend on total pressure. Therefore, MIF in this step would not produce the pressure dependence of $\Delta^{17}\text{O}$ (Fig. 3). Reactions (–a) and (b) diminish in importance as pressure rises

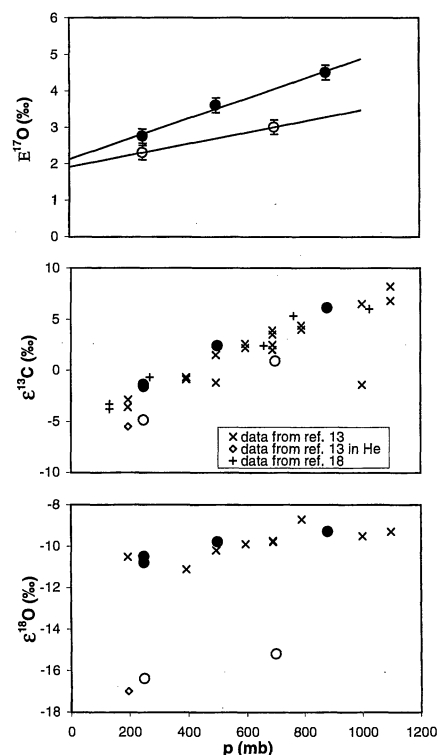


Fig. 3. All isotope fractionation constants for the system CO + OH as a function of total pressure. For ^{13}C and ^{18}O , $\varepsilon^{13}\text{C} = (^{12}\text{k}/^{13}\text{k} - 1)$ and $\varepsilon^{18}\text{O} = (^{16}\text{k}/^{18}\text{k} - 1)$, where k are the overall rate constants for the isotopes with mass i . In analogy to $\Delta^{17}\text{O}$, $E^{17}\text{O}$ is defined as $E^{17}\text{O} \equiv \varepsilon^{17}\text{O} - 0.52 \times \varepsilon^{18}\text{O}$. A moderate but definite pressure dependence of $E^{17}\text{O}$ is observed. The results for ^{13}C and ^{18}O agree well with earlier studies (13, 18). The variable p is pressure in millibars. Filled circles, CO in a bath gas of N_2 or $\text{N}_2 + \text{O}_2$, open circles, CO in a bath gas of He.

because of the increasing competition from reaction step (c). Therefore, MIF in (–a) or (b) cannot explain increasing $\Delta^{17}\text{O}$ with increasing pressure either. Only MIF caused by isotope-selective quenching of HOCO^\ddagger in reaction step (c) would cause the $\Delta^{17}\text{O}$ values to increase with increasing pressure. However, in contrast to the observations, $\Delta^{17}\text{O}$ values should then vanish in the low-pressure limit, where $k = (k_a \times k_b)/(k_{-a} + k_b)$. Very effective quenching of HOCO^\ddagger by H_2O and H_2O_2 could cause a discrepancy between the observed total pressure changes and the actual HOCO^\ddagger quenching rate changes. However, even given the high quenching efficiency of H_2O [~ 10 times that of N_2 (23)], this mechanism seems insufficient to explain the low-pressure offset. Therefore, the established reaction mechanism for $\text{CO} + \text{OH}$ indicates that MIF is produced in at least two elementary reaction steps, one of them being step (c), which induces the positive pressure dependence.

No theoretical explanation for the occurrence of MIF in $\text{CO} + \text{OH}$ is available. It is questionable whether the recent theory that relates MIF to symmetry restrictions in the formation of certain complexes (24) can be directly applied to the reaction $\text{CO} + \text{OH}$. Nota bene, MIF in the important reaction $\text{O} + \text{O}_2 \rightarrow \text{O}_3$ also remains unexplained (25). Here, the rate coefficient for $^{16}\text{O} + ^{18}\text{O}^{18}\text{O}$ is 50% higher than the one for $^{18}\text{O} + ^{16}\text{O}^{16}\text{O}$.

MIF has been detected in each one of the important atmospheric trace gases O_3 , CO_2 , N_2O , and CO . As we now know the origin of MIF in CO , the effect promises to be useful in atmospheric chemistry, as nearly all sources introduce CO into the atmosphere with $\Delta^{17}\text{O} = 0$. Because of the sink reaction $\text{CO} + \text{OH}$, $\Delta^{17}\text{O}$ values increase, which makes MIF a direct measure for the aging of atmospheric CO by exposure to OH .

References and Notes

- J. Bigeleisen, *Science* **147**, 463 (1965); — and M. Wolfsberg, *Adv. Chem. Phys.* **1**, 15 (1958); H. C. Urey, *J. Chem. Soc. London* **1947**, 562 (1947).
- K. Mauersberger, *Geophys. Res. Lett.* **14**, 80 (1987).
- M. H. Thiemens and J. E. Heidenreich, *Science* **219**, 1073 (1983).
- R. K. Yoo and G. I. Gellene, *J. Chem. Phys.* **105**, 177 (1996); J. J. Colman *et al.*, *Science* **273**, 774 (1996).
- T. Röckmann *et al.*, *J. Geophys. Res.* **103**, 1463 (1998).
- J. C. Johnston and M. H. Thiemens, *ibid.* **102**, 25395 (1997); D. Krankowsky *et al.*, *Geophys. Res. Lett.* **22**, 1713 (1995).
- M. H. Thiemens, T. Jackson, K. Mauersberger, B. Schüler, J. Morton, *Geophys. Res. Lett.* **18**, 669 (1991); Y. L. Yung, A. Y. T. Lee, F. W. Irion, W. B. DeMore, J. Wen, *J. Geophys. Res.* **102**, 10857 (1997).
- P. S. Hodder, C. A. M. Brenninkmeijer, M. H. Thiemens, *U.S. Geol. Circ.* **1107** (1994).
- A. K. Huff and M. H. Thiemens, *Eos (Fall Suppl.)* (1996).
- S. S. Cliff and M. H. Thiemens, *Science* **278**, 1774 (1997).
- The δ value is defined as $\delta^{18}\text{O} = (^{18}\text{O}/^{16}\text{O})_{\text{SA}} / (^{18}\text{O}/^{16}\text{O})_{\text{ST}} - 1$ (analogous for ^{17}O), which gives the isotopic ratio of a sample (SA) relative to a standard (ST), in this case Vienna Standard mean ocean water [R. Gonfiantini, *Nature* **271**, 534 (1978)].
- C. A. M. Brenninkmeijer and T. Röckmann, *J. Geophys. Res.* **102**, 25477 (1997).
- C. M. Stevens *et al.*, *Int. J. Chem. Kinet.* **12**, 935 (1980).
- C. A. M. Brenninkmeijer, *J. Geophys. Res.* **98**, 10,595 (1993).
- and T. Röckmann, *Rapid Commun. Mass Spectrom.* **12**, 479 (1998).
- Greenblatt and Howard [G. D. Greenblatt and C. J. Howard, *J. Phys. Chem.* **93**, 1035 (1989)] reviewed the relevant literature and measured the exchange rate coefficient $k_{\text{exch}} < 10^{-15} \text{ cm}^3 \text{ molecule}^{-1} \text{ s}^{-1}$ for the excited HOCO^\ddagger complex, which is 100 times slower than the reaction rate coefficient ($k_{\text{reac}} > 10^{-13} \text{ cm}^3 \text{ molecule}^{-1} \text{ s}^{-1}$) (19). Exchange in the stabilized HOCO radical does not affect the reactants, because HOCO cannot be reconverted to reactants at ambient temperatures (21, 22). Stevens *et al.* (13) measured the same ^{18}O fractionation factor for normal and highly enriched CO in a similar experiment to ours, thus excluding exchange for our conditions.
- M. K. Dubey, R. Mohrschlager, N. M. Donahue, J. G. Anderson, *J. Phys. Chem.* **101**, 1494 (1997).
- H. G. J. Smit, A. Volz, D. H. Ehhalt, H. Knappe, in *Stable Isotopes*, H.-L. Schmidt, H. Förstel, K. Heinzinger, Eds. (Elsevier, Amsterdam, 1982), pp. 147–152.
- W. B. DeMore *et al.*, *JPL Publ.* **11** (1994).
- I. W. M. Smith, *Chem. Phys. Lett.* **49**, 112 (1977).
- M. Mozurkewitch, J. J. Lamb, S. W. Benson, *J. Phys. Chem.* **88**, 6435 (1984).
- D. Fulle, H. F. Hamann, H. Hippler, J. Troe, *J. Chem. Phys.* **105**, 983 (1996).
- G. Paraskevopoulos and R. S. Irwin, *ibid.* **80**, 259 (1983).
- G. I. Gellene, *Science* **274**, 1344 (1996).
- S. M. Anderson, D. Hülsebusch, K. Mauersberger, *J. Chem. Phys.* **107**, 5385 (1997).
- We thank the Atmospheric Environment Service of Canada, the Norwegian Polar Institute, and the Izaña Global Atmospheric Watch observatory for conducting sampling. Supported by the European Commission, DG XII.

23 March 1998; accepted 14 May 1998

A Correlation Between Ultra-Low Basal Velocities in the Mantle and Hot Spots

Q. Williams, J. Revenaugh, E. Garnero*

The statistical correlation between the locations of hot spots at the surface of Earth and the distribution of ultra-low-velocity zones at the base of the mantle has about a 1 percent chance of arising randomly. This correlation is more significant than that between hot spots and negative velocity anomalies in tomographic models of deep mantle compressional and shear velocity. This correlation is consistent with the notion that many hot spots originate in a low-velocity, probably partially molten layer at the core-mantle boundary and undergo little lateral deflection on ascent.

The underlying control on the geographic distribution of hot spots, linear chains of volcanic edifices whose source appears to be fixed relative to surface plate motions, is uncertain. Hot spots tend to be distributed near long-wavelength geoid highs (1) and mid-ocean ridges (2), each of which may in turn be associated with slow seismic velocities in the lower mantle (3, 4). The upwellings that give rise to hot spots are widely thought to originate as instabilities near the core-mantle boundary (CMB) (5, 6), as this region likely represents a major thermal boundary layer. Geophysical observations that support hot spots originating near the CMB have, however, been notably lacking (7), although possible geochemical evidence for such a provenance exists (8). Here we examine whether hot spots are correlated with the presence of recently discovered 5- to 40-km-thick features at the base of Earth's

mantle with compressional wave velocities depressed by as much as 10% from the overlying mantle (9–13). These ultra-low-velocity zones (ULVZs) are likely generated by the presence of partial melt at depth (10, 11); it is unclear whether this partial melt differs chemically from the overlying mantle through (for example) either iron enrichment or volatile enrichment (10).

Thus far, the Fresnel zones of seismic waves sample 44% of the CMB for the presence or absence of ULVZs and ULVZs have been observed to be present over 12% of the CMB (12, 13). The locations of the ULVZs are derived from diffracted compressional wave segments traveling along the mantle side of the CMB (9, 12, 14) and from reflected compressional waves that sample the upper boundary of this basal layer (11, 13) (Fig. 1). Where ULVZs have been detected, their thicknesses are > 5 km; thinner zones may be present elsewhere, but an ~ 5 -km thickness is required for detection. The thicknesses of the ULVZs vary by up to 40 km over distances of ~ 100 km (and possibly less) (9, 10); as such, the nonobservance of this feature does not preclude the presence of undetected patches

Department of Earth Sciences and Institute of Tectonics, University of California, Santa Cruz, CA 95064, USA.

*Present address: Seismological Laboratory, University of California, Berkeley, CA 94720, USA.